EXTRA nephron Journals

Nephron Extra 2011;1:55–68
DOI: 10.1159/000330898
Published online: September 22, 2011

Original Paper

Quantitative Estimation of Urate Transport in Nephrons in Relation to Urinary Excretion Employing Benzbromarone-Loading Urate Clearance Tests in Cases of Hyperuricemia

Toru Nakamura[a, b] Rie Nishi[a] Tuneo Tanaka[a] Kazutaka Takagi[a]
Taro Yamashita[b] Takahiro Yamauchi[a] Takanori Ueda[a]

[a]Department of Medicine, Faculty of Medical Sciences, University of Fukui, Matsuoka, and
[b]Hayashi General Hospital, Echizen, Japan

Key Words
Benzbromarone · Benzbromarone-loading urate clearance test · Four-component system · Urate clearance · Urate transport · Urate underexcretion · Urinary urate excretion

Abstract
Background: A four-component system for urate transport in nephrons has been proposed and widely investigated by various investigators studying the mechanisms underlying urinary urate excretion. However, quantitative determinations of urate transport have not been clearly elucidated yet. ***Methods:*** The equation $C_{ua} = \{C_{cr}(1 - R_1) + TSR\}(1 - R_2)$ was designed to approximate mathematically urate transport in nephrons, where R_1 = urate reabsorption ratio; R_2 = urate postsecretory reabsorption ratio; TSR = tubular secretion rate; C_{ua} = urate clearance, and C_{cr} = creatinine clearance . To investigate relationships between the three unknown variables (R_1, R_2, and TSR), this equation was expressed as contour lines of one unknown on a graph of the other two unknowns. Points at regular intervals on each contour line for the equation were projected onto a coordinate axis and the high-density regions corresponding to high-density intervals of a coordinate were investigated for three graph types. For benzbromarone (BBR)-loading C_{ua} tests, C_{ua} was determined before and after oral administration of 100 mg of BBR and C_{ua}BBR(●●) was calculated from the ratio of C_{ua}BBR(100)/C_{ua}. ***Results:*** Before BBR ad-

This study has been approved by the Ethics Committee of the Hayashi General Hospital (Director: Dr. M. Nojiri).

Toru Nakamura
Department of Medicine, Faculty of Medical Sciences
University of Fukui
Matsuoka, Fukui 910-1193 (Japan)
Tel. +81 776 61 3111, E-Mail nakamura.tooru@beige.plala.or.jp

KARGER

Nephron Extra 2011;1:55–68
DOI: 10.1159/000330898
Published online: September 22, 2011

www.karger.com/nne

ministration, points satisfying the equation on the contour line for $R_1 = 0.99$ were highly dense in the region $R_2 = 0.87–0.92$ on all three graphs, corresponding to a TSR of 40–60 ml/min in hyperuricemia cases (HU). After BBR administration, the dense region was shifted in the direction of reductions in both R_1 and R_2, but TSR was unchanged. Under the condition that $R_1 = 1$ and $R_2 = 0$, urate tubular secretion (UTS) was considered equivalent to calculated urinary urate excretion (U_{ex}) in a model of intratubular urate flow with excess BBR; C_{ua}BBR(●●) = TSR was deduced from the equation at $R_1 = 1$ and $R_2 = 0$. In addition, TSR of the point under the condition that $R_1 = 1$ and $R_2 = 0$ on the graph agreed with TSR for the dense region at excess BBR. TSR was thus considered approximately equivalent to C_{ua}BBR(●●), which could be determined from a BBR-loading C_{ua} test. Approximate values for urate glomerular filtration, urate reabsorption, UTS, urate postsecretory reabsorption (UR_2), and U_{ex} were calculated as 9,610; 9,510; 4,490; 4,150, and 440 μg/min for HU and 6,890; 6,820; 4,060; 3,610, and 520 μg/min for normal controls (NC), respectively. The most marked change in HU was the decrease in TSR (32.0%) compared to that in NC, but UTS did not decrease. Calculated intratubular urate contents were reduced more by higher UR_2 in HU than in NC. This enhanced difference resulted in a 15.4% decrease in U_{ex} for HU. ***Conclusion:*** Increased UR_2 may represent the main cause of urate underexcretion in HU.

Introduction

Urinary urate is excreted via a complicated combination of urate transport in nephrons [1–3]. Earlier studies on urate transport in nephrons, including micropuncture, microinjection, and microperfusion experiments, have indicated that urate is filtered freely at the glomerulus [4–6], and intratubular urate contents are adjusted following bidirectional urate transport, including reabsorptions and secretion [1, 2, 7]. To analyze the mechanisms underlying urinary urate excretion, a four-component system has been investigated and endorsed by various investigators [1, 5, 8–11]. According to that system, most of the urate filtered through the glomerulus [urate glomerular filtration (UGF)] is considered to be reabsorbed [(urate reabsorption (UR_1)] at proximal sites of the tubules, and residual urate contents in intratubular fluid are supplemented by urate tubular secretion (UTS) [12, 13]. Considerable amounts of secreted urate are thought to be reabsorbed in urate postsecretory reabsorption (UR_2) [9, 14, 15]. Quantitative analysis of the amount of each fraction, i.e. UGF, UR_1, UTS, and UR_2, as well as calculated urinary urate excretion (U_{ex}), has been performed using probenecid and pyrazinamide, and ratios of each fraction have been estimated as approximately 99, 50, 40, and 10% of UGF, respectively [1, 2, 16]. To analyze the amount of each kind of transport, probenecid has been used as a reabsorption inhibitor and pyrazinamide as a secretion inhibitor. However, the latter has also been reported as a reabsorption accelerator rather than as an inhibitor [17–19]. Contributions of each type of transport have thus to be clearly elucidated in quantitative analyses.

Benzbromarone (BBR) has recently been reported as a major and strong inhibitor of urate transport into epithelial cells of nephrons by strongly inhibiting the URAT1 urate transporter [20]. In addition, findings that BBR does not exert uricosuric effects in patients with hypouricemia caused by damage to URAT1 [21] suggest that the inhibitory effects of BBR are specific to URAT1. Using these characteristics of BBR, we attempted to quantitatively estimate urate transport in nephrons in relation to urinary urate excretion employing the equation $C_{ua} = \{C_{cr}(1 - R_1) + TSR\}(1 - R_2)$ [16], where C_{ua}, R_1, R_2, and TSR are urate clearance, urate reabsorption ratio, urate postsecretory reabsorption ratio, and tubular secretion rate, respectively, without inhibiting urate secretion using pyrazinamide. In parallel with

Nephron Extra 2011;1:55–68
DOI: 10.1159/000330898
Published online: September 22, 2011

www.karger.com/nne

recent progress in urate transporter investigations [20, 22–24], studies on total amounts of urate transport as a summation of the actions of these transporters will also be important for understanding the mechanisms of urinary urate excretion in human subjects, particularly in patients with hyperuricemia (HU).

Materials and Methods

Subjects comprised 20 male gouty patients with HU (age range, 22–62 years) showing serum urate concentration (S_{ua}; >7.0 mg/dl), together with 10 male volunteers as normal controls (NC; age range, 21–44 years). Administration of all medication affecting S_{ua}, such as BBR, probenecid, allopurinol, diuretics, losartan, fenofibrate, and nucleoside derivatives, was discontinued for at least 2 weeks prior to experiments. All patients provided written informed consent. For BBR-loading C_{ua} tests, a single dose of 100 mg of BBR was administered orally and urine fractions were collected 60 to 0 min before and 180 to 240 min after BBR administration [16]. Blood samples were collected 30 min before and 210 min after BBR administration. Urate and creatinine concentrations in urine fractions and blood samples were determined using a multichannel autoanalyzer (type 7180; Hitachi, Tokyo) that employed automation of uricase peroxidase and creatininase peroxidase procedures, respectively. C_{ua} and C_{cr} were calculated as reported previously [16, 25, 26] before and after BBR administration, and are expressed assuming a standard body surface area of 1.73 m^2.

Quantitative Expression of Urate Transport in Nephrons Using an Equation

The equation $U_{ex} = \{C_{cr} \cdot S_{ua}(1 - R_1) + UTS\}(1 - R_2)$ was designed to calculate urate transport by secretion and reabsorption in relation to urinary urate excretion based on a four-component system [16]. Since UTS could be expressed as TSR S_{ua}, because UTS has been shown to be influenced by urate concentration in the circulating blood in the kidney in microinjection and microperfusion experiments [27], we obtained

$$C_{ua} = \{C_{cr}(1 - R_1) + TSR\}(1 - R_2) \quad (1)$$

For calculating urate transport using this equation, the following assumptions were set after referring to previous reports of experimental data:

(1) urate passed through the glomerular membrane without any loss or retention [4–6];
(2) 99% of UGF was reabsorbed at proximal sites of tubules when BBR was not administered [1, 2];
(3) BBR strongly inhibited reabsorptions [20, 21] (R_1 and R_2), but did neither inhibit TSR nor C_{cr} in the BBR-loading C_{ua} test;
(4) urate concentration in tubular secretion fluid was proportional to S_{ua} [27], and
(5) levels of UR_2 were proportional to intratubular urate contents.

Estimation of C_{ua}BBR(●●)

Effects of oral doses of BBR on the C_{ua} curve determined by the C_{ua} test [16] were simulated using the exponential equation $y = b - c \cdot e^{-ax}$, where y is C_{ua}, x is BBR dose, and a, b, and c are constants [16]. Constants a, b, and c were calculated by applying the least-square method as 0.0090, 45.6, and 40.5 for HU and 0.0081, 80.1, and 70.2 for NC, respectively. The ratio of C_{ua}BBR(100)/C_{ua}BBR(●●) on the curve was calculated as 0.639 for HU and 0.610 for NC, where C_{ua}BBR(100) is C_{ua} after administration of 100 mg BBR. Accordingly, C_{ua}BBR(●●) could be calculated as C_{ua}BBR(100)/0.639 for HU and C_{ua}BBR(100)/0.610 for NC [16].

Nephron Extra 2011;1:55–68
DOI: 10.1159/000330898
Published online: September 22, 2011

www.karger.com/nne

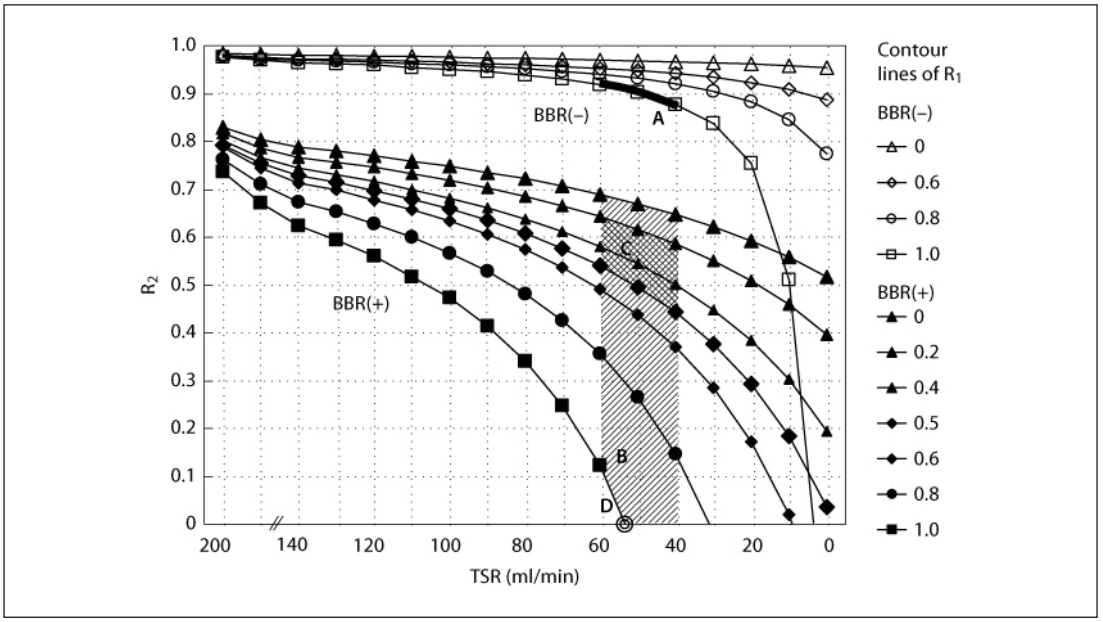

Fig. 1. Investigation of condensed site of location of points corresponding to the equation $C_{ua} = \{C_{cr} (1 - R_1) + TSR\}(1 - R_2)$ as a contour line of R_1 on R_2 versus TSR plot as variables in HU. Area A = Without BBR; areas B/C = excess BBR; point D = tentatively under the condition of $R_1 = 1$ and $R_2 = 0$. C_{ua} values of 4.9 ml/min at BBR(–) and 52.6 ml/min at excess of BBR, respectively.

Results

Graphic analysis of the relationship between R_1, R_2, and TSR was performed in the equation,

$$C_{ua} = \{C_{cr}(1 - R_1) + TSR\}(1 - R_2).$$

The equation was plotted as contour lines for one of the three unknowns (R_1, R_2, or TSR) on graphs with the other two unknowns as variables. Any number of contour lines and points satisfying the equation could be plotted, but the points at regular intervals on contour curves were particularly dense with respect to a coordinate within a certain region. The scale of the coordinates for this dense region and the values of the contour line could indicate closer relationships between R_1, R_2, and TSR.

Without BBR Administration

R_2-versus-TSR Graph. Using equation 1, contour lines of R_2 versus TSR with respect to several values of R_1 were plotted. Coordinates of TSR were limited to <200 ml/min, since higher values would not be encountered under usual conditions. The contour lines of the equation lay within the graph area for $R_1 = 0$–1.0. R_1 was assumed to be 0.99 without BBR administration; the R_2 values on the contour line for $R_1 = 0.99$ ranged from 0 to nearly 1.0, and the range for the dense region was from $R_2 = 0.87$ to nearly 1.0 in HU. The corresponding TSR range for the dense region was >40 ml/min (fig. 1).

R_1-versus-TSR Graph. Using equation 1, contour lines of R_1 versus TSR with respect to several values of R_2 were plotted. Almost all points in the graph area could be reached by a contour line, except a small area above the $R_2 = 0$ contour line. On the line $R_1 = 0.99$, corresponding to the condition without BBR administration, all TSR values in the range >5 ml/

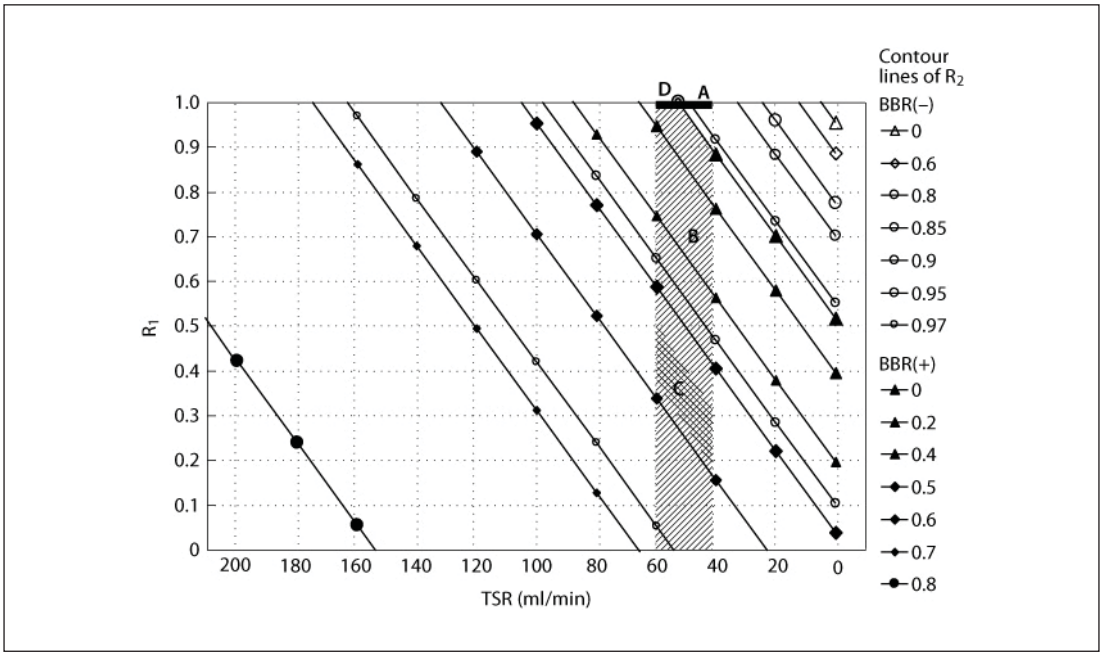

Fig. 2. Investigation of condensed site of location of points corresponding to the equation $C_{ua} = \{C_{cr} (1 - R_1) + TSR\}(1 - R_2)$ as a contour line of R_2 on R_1 versus TSR plot as variables in HU. Area A = Without BBR; areas B/C = excess BBR; point D = tentatively under the condition of $R_1 = 1$ and $R_2 = 0$. C_{ua} values of 4.9 ml/min at BBR(–) and 52.6 ml/min at excess of BBR, respectively.

min could be reached. However, contour lines were dense in the range of $R_2 = 0–0.92$ in HU. The corresponding TSR range for this dense area was 5–60 ml/min (fig. 2).

R_1-versus-R_2 Graph. Using equation 1, contour lines of R_1 versus R_2 with respect to several values of TSR were also plotted. All points above the TSR = 0 contour line could be reached. For $R_1 = 0.99$, this included the full range of R_2, but contour lines with respect to TSR were particularly dense in the narrow range $R_2 = 0.87$ to nearly 1.0 in HU. The corresponding TSR values of the contour lines through this R_2 range were from 40 to 200 ml/min (fig. 3).

In the above three graphic analyses of the relationships between R_1, R_2, and TSR, while BBR was not administered, the common location of the dense R_2 range on the $R_1 = 0.99$ line showed good agreement in the R_2-versus-TSR and R_1-versus-R_2 graphs. The range was $R_2 = 0.87$ to nearly 1.0. However, contour lines were not dense in the R_1-versus-TSR graph with respect to TSR, so that density in the R_2 direction was decreasing in inverse proportion to increasing TSR volume. Dense regions with respect to projection onto a coordinate axis of regular intervals of points on each contour line must be for all three graphic analyses, thus involving all three unknowns; that is, it is not sufficient that points be dense for some coordinate in two of the graphs but not in the third. Only within the narrow region $R_2 = 0.87–0.92$ on the line $R_1 = 0.99$ are the points dense in all three graphic analyses. The corresponding TSR range was 40–60 ml/min. In this region, solutions to equation 1 are most dense with respect to all three unknowns. This region was thus considered the most probable location for points corresponding to the equation in HU (area A on each graph, fig. 1–3).

Graphic analyses were undertaken in the same manner in NC. The most probable regions for R_1, R_2, and TSR were calculated as 0.99, 0.86–0.88, and 70–90 ml/min, respectively.

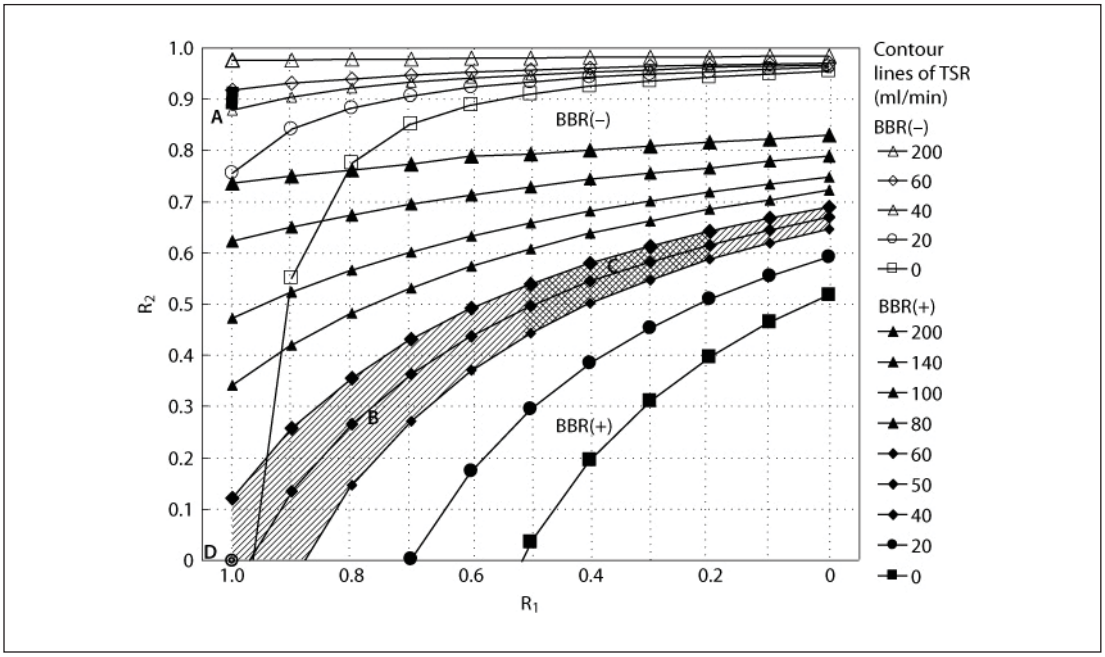

Fig. 3. Investigation of condensed site of location of points corresponding to the equation $C_{ua} = \{C_{cr} (1 - R_1) + TSR\}(1 - R_2)$ as a contour line of TSR on R_1 versus R_2 plot as variables in HU. Area A = Without BBR; areas B/C = excess BBR; point D = tentatively under the condition of $R_1 = 1$ and $R_2 = 0$. C_{ua} values of 4.9 ml/min at BBR(–) and 52.6 ml/min at excess of BBR, respectively.

After BBR Administration

With BBR administration, R_1 and R_2 were reduced, but TSR was unchanged, as inhibitory actions of BBR are considered specific to URAT1 [20, 28]. In addition, C_{cr} in the glomerulus, which corresponds to TSR in tubules, was also unchanged during BBR-loading C_{ua} tests. Accordingly, contour lines were shifted parallel to the R_1 and R_2 axes on the graphs, but were not moved along the TSR axis. When BBR doses were increased, C_{ua} was also increased in a dose-dependent manner [16]. At excess of BBR, equation 1 could be rewritten as follows:

$$C_{ua}BBR(\bullet\bullet) = [C_{cr}\{1 - R_1(\bullet\bullet)\} + TSR]\{1 - R_2(\bullet\bullet)\} \quad (2)$$

Shift of the site of dense points on contour lines of equation 1 from BBR = 0 to excess BBR was investigated on the three graphs in the same manner as cases without BBR.

R_2-versus-TSR Graph. Contour lines of R_1 were shifted parallel to the R_2 axis and intervals widened. Area A was also shifted parallel to the R_2 axis and could reach area B (between the contour lines for $R_1 = 0$ and $R_1 = 0.99$ with BBR). The corresponding R_2 was from 0 to 0.68. Kramp and Lenoir [29] performed micropuncture and microperfusion experiments showing that in BBR-pretreated rats, the inhibition rate of UR_1 at proximal sites of tubules was faster and higher compared to distal sites. Referring to these data, the range of area B could be further reduced. Furthermore, the rate of inhibition of UR_1 at excess BBR might not be complete due to the existence of other kinds of urate transporters [22, 30] that might be less inhibited by BBR than URAT1 [20, 21]. The region in which points at regular intervals on contour lines of equation 2 projected onto a coordinate axis were most dense could thus be speculated to lie probably closer between $R_1 = 0.2$ and $R_1 = 0.5$ with excess BBR, so the corresponding R_2 was calculated from equation 2 as 0.44–0.64 and the corresponding TSR was 40–60 ml/min in HU (area C, fig. 1).

Nephron Extra 2011;1:55–68
DOI: 10.1159/000330898
Published online: September 22, 2011

www.karger.com/nne

R_1-versus-TSR Graph. The contour lines of R_2 shifted parallel to the R_1 axis and intervals widened. Area A also shifted parallel to the R_1 axis and reached area C (between $R_1 = 0.2$ and $R_1 = 0.5$ with BBR), as speculated above. The corresponding R_2 and TSR values were 0.54–0.59 and 40–60 ml/min, respectively, in HU (fig. 2).

R_1-versus-R_2 Graph. Contour lines of TSR were moved with respect to both the R_1 and R_2 axes, and became more diagonal and intervals widened, as before. Area A was also shifted diagonally and reached area C, as speculated above. The corresponding R_2 and TSR values were 0.44–0.64 and 40–60 ml/min, respectively, in HU (fig. 3).

These findings on analysis at excess BBR suggest that solutions to equation 2 were most dense in area C, where R_1, R_2, and TSR were estimated to be 0.2–0.5, 0.54–0.59, and 40–60 ml/min in HU and 0.2–0.5, 0.48–0.54, and 70–90 ml/min in NC, respectively.

Relationship between TSR and C_{ua}BBR(●●)

A point corresponding to the condition of $R_1 = 1$ and $R_2 = 0$ at excess BBR was introduced on the three graphs and shown as point D (double circles in fig. 1–3, respectively), where the situation of urate transport could be explained, so that UGF was completely reabsorbed and UTS did not receive any reabsorption in the intratubular urate flow model [16]. If U_{ua}BBR(●●) were determined under this condition, then U_{ua}BBR(●●) would correspond to UTS, so C_{ua}BBR(●●) would correspond to TSR. Point D and area C, where points corresponding to equation 2 were dense, were separated from each other on the graphs, but both showed relationships between R_1, R_2, and TSR under the same condition of C_{ua}BBR(●●) with excess of BBR. TSR could thus be deduced from C_{ua}BBR(●●) at $R_1 = 1$ and $R_2 = 0$ in equation 2. The three graphs showed that TSR of point D was in the same range as TSR of area C, namely 40–60 ml/min. TSR was thus considered approximately equivalent to C_{ua}BBR(●●). TSR of point D was also equivalent to that of area A. Using C_{ua}BBR(100), an approximation of TSR was obtained from equation 2 as follows:

$$TSR = C_{ua}BBR(●●) - 0.01 \cdot C_{cr}$$
$$TSR = C_{ua}BBR(100)/0.639 - 0.01 \cdot C_{cr}$$
$$TSR = 51.6 \text{ for HU and}$$
$$TSR = 75.9 \text{ for NC}$$

Accordingly, R_2 could be calculated from equation 2 as follows:

$$R_2 = 1 - C_{ua}/(0.01 \cdot C_{cr} + TSR)$$
$$R_2 = 0.905 \text{ for HU and}$$
$$R_2 = 0.872 \text{ for NC}$$

Equations for estimating urate transport and urinary urate excretion are summarized in table 1.

Inhibition of R_1 and R_2 by BBR

When BBR was administered, the region of highly dense points of equation 1 was considered to be shifted from area A to area B, and more probably to area C at excess BBR on the graphs. R_1 in area B could be distributed within $R_1 = 0–0.99$ and that in area C could be reduced to $R_1 = 0.2–0.5$, as speculated above in each stage of BBR dose. The range of R_2 in area C could be calculated from equation 1 at each BBR dose using the corresponding C_{ua} (fig. 4). Estimates of R_2, shown by the middle point of area C, remained in the upper region of the R_2 range and gradually decreased with increasing BBR doses. With excess BBR, R_2 reached around 0.58. Area C could be selected in a narrow range, as the contour lines were crowded in the upper region of area B. The corresponding mean R_1 in area C decreased rapidly to an area between $R_1 = 0.3$ and $R_1 = 0.4$ at 25 mg of BBR, which was continued until excess of BBR.

Nephron Extra 2011;1:55–68
DOI: 10.1159/000330898
Published online: September 22, 2011

www.karger.com/nne

Table 1. Equations for approximating urate transport and urinary urate excretion without BBR administration

Equation	Unit
$C_{ua} = \{C_{cr}(1 - R_1) + TSR\}(1 - R_2)$	
$C_{ua}BBR(●●) = C_{ua}BBR(100)/\alpha$	ml/min
$TSR = C_{ua}BBR(100)/\alpha - 0.01 \cdot C_{cr}$	ml/min
$R_2 = 1 - C_{ua} \cdot \alpha / C_{ua}BBR(100)$	(ratio)
$UGF = S_{ua} \cdot C_{cr}$	μg/min
$UTS = TSR \cdot S_{ua}$	μg/min
$UR_2 = (0.01\ UGF + UTS) \cdot R_2$	μg/min
$U_{ex} = 0.01\ UGF + UTS - UR_2$	μg/min

See text for abbreviations. α was replaced by 0.610 and 0.639 for NC and HU, respectively.

Table 2. Urate transport in nephrons and urinary excretion in hyperuricemia

	BBR-loading C_{ua} tests						Approximate urate transport in nephrons					U_{ex}
	S_{ua}	U_{ua}	C_{ua}	C_{cr}	R	$C_{ua}BBR$	UGF	UTS	TSR	UR_2	R_2	
HU (n = 20)												
Mean	87.7	6.00	4.90	109.2	4.57	33.7	9,610	4,490	51.6	4,150	0.905	440
SD	10.4	1.57	1.13	14.5	1.25	7.5	2,110	990	11.6	940	0.022	110
SE	2.3	0.35	0.25	3.2	0.28	1.7	470	220	2.6	210	0.005	25
NC (n = 10)												
Mean	53.4	7.66	9.80	129.6	7.60	47.1	6,890	4,060	75.9	3,610	0.872	520
SD	6.5	0.95	1.13	10.0	1.06	5.7	700	710	9.3	660	0.015	80
SE	2.0	0.30	0.36	3.2	0.33	1.8	220	220	3.0	210	0.005	25
p value							<0.0001	0.055	<0.0001	0.009	<0.0001	0.0002

$C_{ua}BBR$ = C_{ua} after administration of 100 mg of BBR. S_{ua}: μg/ml; U_{ua}: μg/kg/min; C_{ua}: ml/min/1.73 m^2; UGF, UTS: μg/min; TSR: ml/min/1.73 m^2; UR_2, U_{ex}: μg/min.

Marked differences between inhibition patterns of R_1 and R_2 by single administration of BBR represented an interesting finding.

Estimated Urate Transport Amounts in Nephrons and Urinary Excretion in HU

Urate transport amounts in approximation of UGF, UR_1, UTS, UR_2, and U_{ex} were calculated using the equations in table 1 and are shown in table 2. Ratios of each transport to UGF in HU and NC were comparable to those reported previously [1, 2], and ratios of UTS, UR_2, and U_{ex} to UGF in HU were significantly lower than those in NC (fig. 5).

Comparing urate transport and intratubular urate contents in nephrons between HU and NC, UGF was significantly higher in HU (39.5%) than in NC, but the difference in intratubular urate contents was minimal at the UR_1 stage. TSR in HU was significantly lower (32.0%) compared to that in NC, but UTS in HU was slightly higher (10.6%) than that in NC, and intratubular urate contents in HU were also slightly higher than those in NC at the UTS stage (11.1%). UR_2 in HU was significantly higher (15.0%) than that in NC. Since UR_2 corresponded to approximately 90% of intratubular urate contents at the stage, residual intratubular urate contents were greatly influenced by the small difference in UR_2 between HU and NC. Intratu-

Nephron Extra 2011;1:55–68
DOI: 10.1159/000330898
Published online: September 22, 2011

www.karger.com/nne

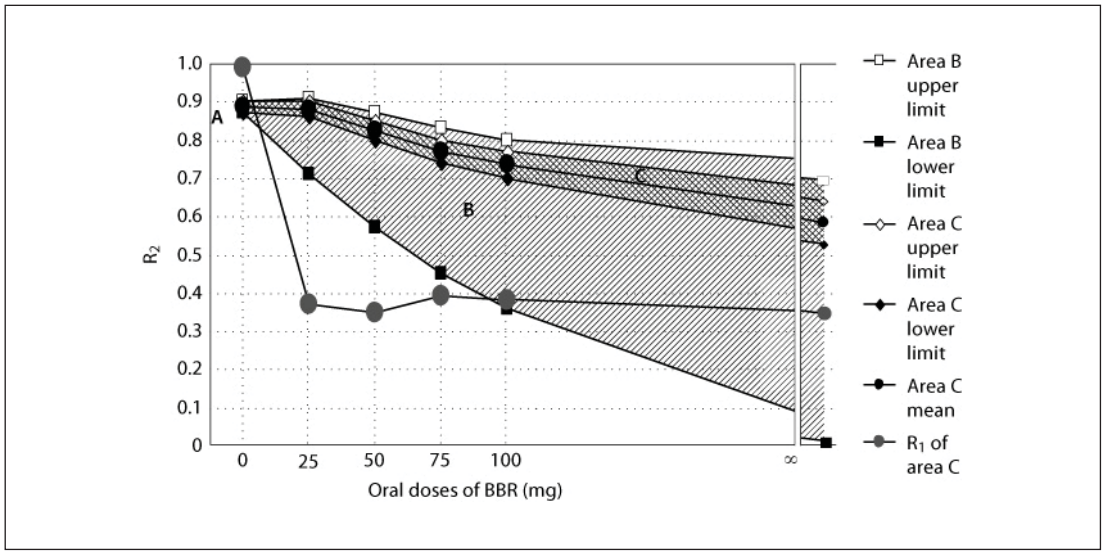

Fig. 4. Inhibition of R_1 and R_2 by BBR. Area A = Without BBR; area B = ranging between $R_1 = 0$ and R = 0.99 at BBR(+); area C = ranging between $R_1 = 0.5$ and R = 0.2 at BBR(+). R_2 and corresponding R_1 were calculated from equation 1. From mean of R_2 in area C, R_1 in area C was also calculated using the equation and was expressed using scale of R_2.

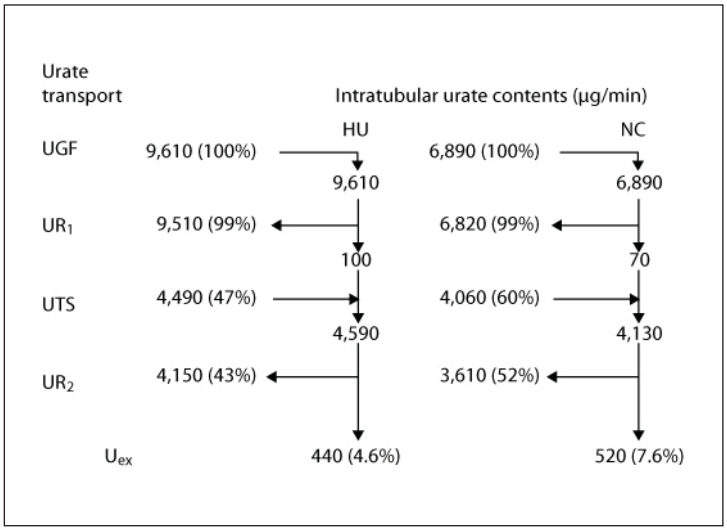

Fig. 5. Comparison of urate transport and intratubular urate contents between HU and NC. UGF: μg/min, and UR_1, UTS, UR_2, and U_{ex}: μg/min.

bular urate contents in HU had been higher than those in NC from the stage of UGF to UTS, even with large variations present, but urate contents showed an inverse relationship at the UR_2 stage. Subsequently, U_{ex} in HU was 15.4% lower than that in NC, suggesting that higher UR_2 in HU than in NC represents the crucial factor for reducing U_{ex}, rather than significantly higher UGF in HU compared to that in NC (fig. 5). R_2 in HU was only 3.8% higher than that in NC, but intratubular urate contents were supposed to be elevated by increased UTS and were enlarged to 15.4% at the UR_2 stage, suggesting that elevation of intratubular urate contents by addition of increased UTS in HU resulted in enhancement of increased UR_2 and subsequently induced enhancement of the rate of urate underexcretion (15.4%) in HU.

EXTRA nephron Journals
Nephron Extra 2011;1:55–68
DOI: 10.1159/000330898
Published online: September 22, 2011

www.karger.com/nne

Discussion

In this study, quantitative estimations of urate transport and intratubular urate contents in nephrons were investigated in relation to urinary urate excretion based on the four-component system by designing the equation $C_{ua} = \{C_{cr}(1 - R_1) + TSR\}(1 - R_2)$, using assumptions introduced by previous reports of experimental data. High-density regions with respect to the projection onto a coordinate axis of points at regular intervals on contour lines of this equation were analyzed on graphs plotted for two of three unknowns (R_1, R_2, and TSR) as variables, with the remaining unknown used to determine the contour line, so that densities and locations of these points on the contour lines of the equation could indicate the relationships of the three unknowns. R_1 was assumed to be 0.99 before BBR administration and the R_2 values of points satisfying the equation were highly dense in a narrow R_2 range, which was regarded as the probable value of R_2. With BBR administration, contour lines were shifted parallel to the R_1 or R_2 axes, but not to the TSR axis. C_{ua}BBR(●●) was considered equivalent to TSR from the intratubular urate flow model in the nephron, as well as from deduction of the relationship that C_{ua}BBR(●●) = TSR from equation 2 under condition of $R_1 = 1$ and $R_2 = 0$. TSR could thus be estimated by BBR-loading C_{ua} tests. Urate transport coefficients estimated by calculations in our laboratory were comparable to previously reported data [1, 2].

R_2 was slightly higher in HU than in NC (3.8%). This difference was enhanced to 15.0% at the UR_2 stage by increases in UTS, resulting in a 15.4% decrease in U_{ex} for HU compared to that for NC. If significant decreases in TSR in HU were unaccompanied by hyperuricemia, U_{ex} in HU would be further decreased. As an example, if S_{ua} in HU was 5.3 mg/dl (the same as S_{ua} in NC), UGF, UTS, UR_2, and U_{ex} in HU could be calculated as 5,780; 2,730; 2,520, and 270 μg/min, respectively, and the decrease in U_{ex} in HU would be markedly higher than that in NC. Since significant decreases in TSR among HU were observed widely in frequency and highly in grade from the early stage of gouty patients and TSR was placed in the upper reaches of intratubular urate flow in nephrons compared to UR_2, hyperuricemia was suggested to originate with an initial decrease in TSR, producing urate underexcretion and subsequently resulting in urate retention and hyperuricemia. Accordingly, decreased TSR would be a fundamental phenomenon for HU, and hyperuricemia could be considered as a reasonable reaction toward recovering from the decrease of U_{ex} in HU. Actually, the decreased U_{ex} that might be induced by decreased TSR was well compensated by hyperuricemia (table 2).

Analyzing the relationships between R_1, R_2, and TSR in equation 1, regular points satisfying the equation on the contour line of $R_1 = 0.99$ were more dense in a certain small R_2 range that could be understood more easily when projected onto the R_2 axis. The dense region was considered to represent a region in which solutions to the equation were most dense, so solutions were located in this region most frequently in the sense of a probability distribution. Similar reasoning could be used to consider the common R_2 values appearing in all three graphic analyses as the most dense region with respect to R_1, R_2, and TSR. This region is the most frequent in terms of probability. In other regions, the probability was reduced because of low density. Since dense areas in the graphs could select a narrow range of R_2 and TSR, we considered these to be the areas where the equation best approximated the relationship between the three unknowns.

In an analysis of the high-density region corresponding to the equation after BBR administration, area C was designated as meeting the condition that R_1 was lower than R_2 on BBR inhibition, referring to Kramp's experiments. The data satisfying this condition also coincided with histochemical findings reported by Enomoto et al. [20], and Enomoto and Endou [28], who reported that URAT1 was more frequently located in proximal sites than in distal sites of tubular epithelial cells. Other kinds of experiments in cultured cells have sug-

Nephron Extra 2011;1:55–68
DOI: 10.1159/000330898
Published online: September 22, 2011

www.karger.com/nne

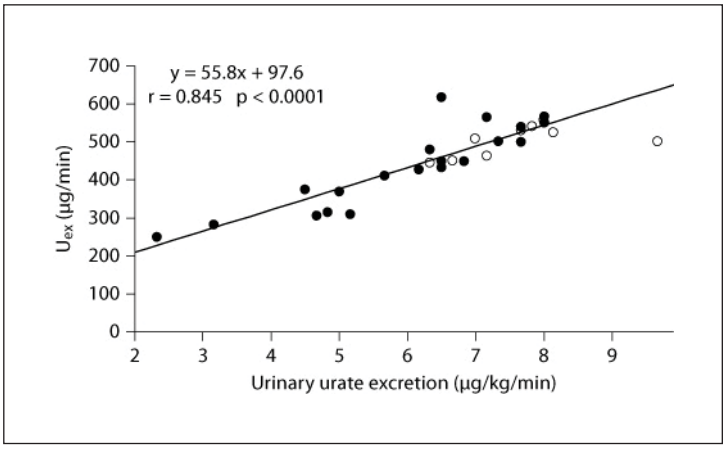

Fig. 6. Correlation between urinary urate excretion and U_{ex}. ● = HU; ○ = NC.

gested that the inhibition rate of UR_1 at BBR-saturated concentrations was around 55% [30]. Inhibition of UR_1 might not reach the level of complete inhibition even with excess BBR due to the potential presence of transporters other than URAT1 [20, 22] despite the higher affinity of this transporter for BBR. The high-density region corresponding to the equation was thus considered to be concentrated in area C. The large distance between area C and point D was not reduced at excess BBR, mainly due to the low grade of inhibition on R_2, reflecting the paucity of URAT1 transporters at distal sites in tubules [20].

Equation 1 was designed for investigation of relationships between R_1, R_2, and TSR, but U_{ua} determined by C_{ua} tests and U_{ex} calculated by the equation showed a highly significant correlation ($r = 0.85$, $p < 0.0001$; fig. 6), suggesting that designing equation 1 under our assumptions and using the following calculations could be considered suitable.

Equation 1 was considered under the assumption that UGF, UR_1, UTS and UR_2 were sequential, but some investigators have suggested that reabsorption and secretion could occur simultaneously in the same segment of the proximal tubule [31–33]. In that case, the following equation could be constructed using the same assumptions applied to equation 1 in the intratubular urate flow model [16].

$$U_{ua} = C_{cr} \cdot S_{ua}(1 - R_1) + \Sigma \Delta UTS(1 - R_2)$$

where summation of $\Delta UTS(1 - R_2)$ was assumed to reach UTS_1 to obtain experimental data that $U_{ua} = 6.00$ and 7.66 for HU and NC, respectively, by BBR-loading C_{ua} tests (table 2), then

$$U_{ua} = C_{cr} \cdot S_{ua}(1 - R_1) + UTS_1(1 - R_2)$$
$$U_{ua} = C_{cr} \cdot S_{ua}(1 - R_1) + TSR_1 \cdot S_{ua}(1 - R_2)$$
$$C_{ua} = C_{cr}(1 - R_1) + TSR_1(1 - R_2) \quad (3)$$

After substituting experimental data of table 2 for C_{ua}, C_{cr}, and C_{ua}BBR(●●), graphic analysis of equation 3 was performed in the same manner as in the case of the equation 1, estimating R_1, R_2, and TSR_1 as 0.99, 0.91–0.94 and 40–60 ml/min for HU and 0.99, 0.87–0.90 and 70–90 ml/min for NC, respectively (fig. 7, 8). These findings indicate that the urate transport coefficients are almost the same as in equation 1. Both analyses thus reached the same conclusion that increased postsecretory reabsorption may represent the main cause of urate underexcretion in HU.

Some investigators [34] have reported that secretion might be overestimated in the four-component theory. However, according to our analyses, the possibility seems relatively un-

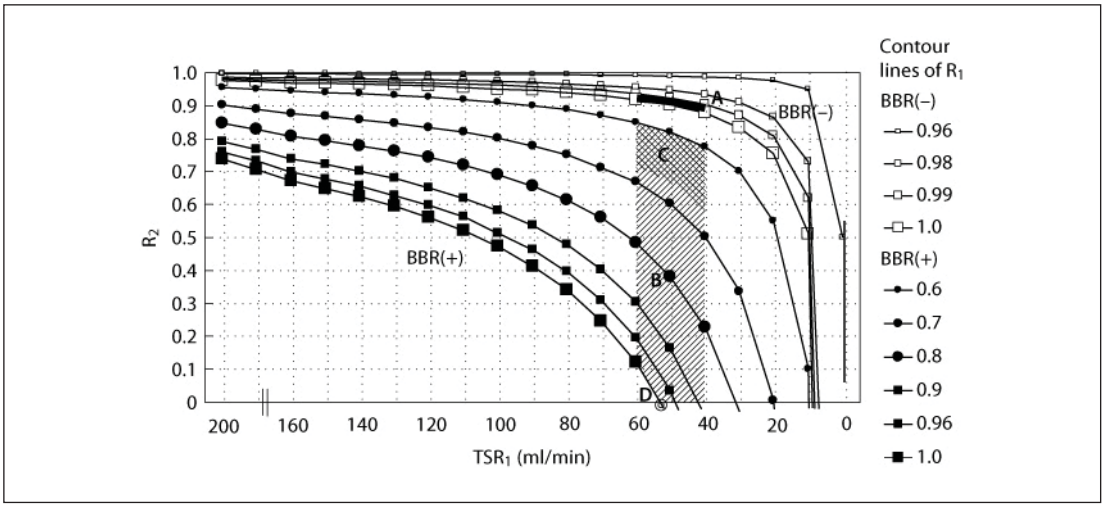

Fig. 7. Investigation of condensed site of locations of points corresponding to the equation $C_{ua} = C_{cr}(1 - R_1) + TSR_1(1 - R_2)$ as a contour line of R_1 on R_2 versus TSR_1 plot as variables in HU in the same manner as the equation $C_{ua} = \{C_{cr}(1 - R_1) + TSR\}(1 - R_2)$ in figure 1. Area A = Without BBR; areas B/C = excess BBR; point D = tentatively under the condition of $R_1 = 1$ and $R_2 = 0$. C_{ua} values were 4.9 ml/min at BBR(–) and 52.6 ml/min at excess of BBR, respectively.

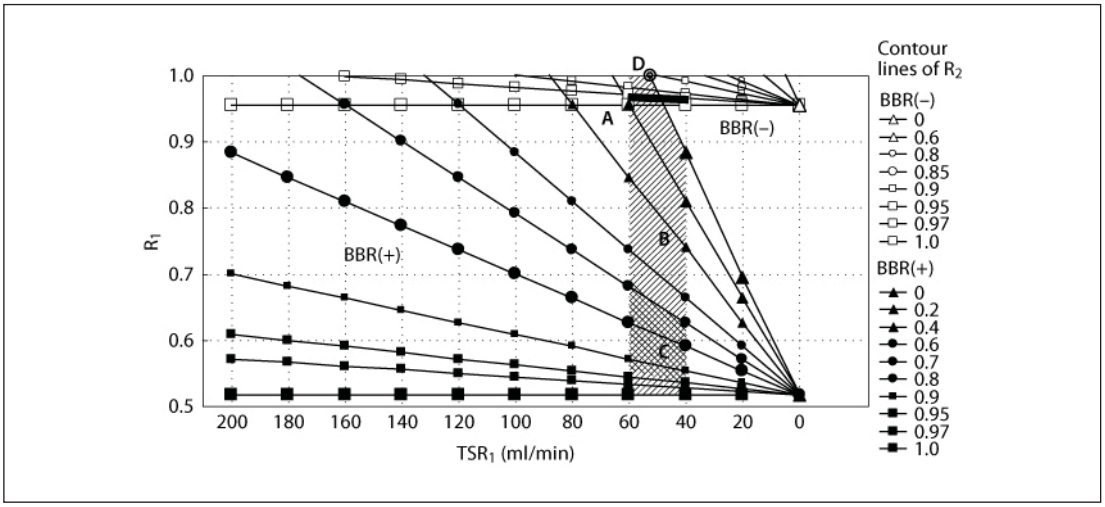

Fig. 8. Investigation of condensed site of location of points corresponding to the equation $C_{ua} = C_{cr}(1 - R_1) + TSR1(1 - R_2)$ as a contour line of R_2 on R_1 versus TSR_1 plot as variables in HU in the same manner as $C_{ua} = \{C_{cr}(1 - R_1) + TSR\}(1 - R_2)$ in figure 2. Area A = Without BBR; areas B/C = excess BBR; point D = tentatively under the condition of $R_1 = 1$ and $R_2 = 0$. C_{ua} values were 4.9 ml/min at BBR(–) and 52.6 ml/min at excess of BBR, respectively.

likely because few corresponding points for both equation 1 and equation 3 were located both in low TSR regions and in low R_2 regions on the graphs.

Studies on quantitative estimation of urate transport in the nephron could result in a more precise understanding of the pathophysiology of urate transport and intratubular flow of urate contents in HU. For example, instead of a significant decrease in TSR among HU compared to that in NC, UTS among HU was higher than that in NC, as the low TSR was

Nephron Extra 2011;1:55–68
DOI: 10.1159/000330898
Published online: September 22, 2011

www.karger.com/nne

compensated by high S_{ua} in HU. The increase in UTS enhanced increases in UR_2, which subsequently enhanced decreases in U_{ex} for HU.

Since cases of hyperuricemia show a large degree of variability in the level of S_{ua} and amount of U_{ua}, as well as in qualities such as overproduction and underexcretion [25, 26, 35], analyses and investigations of greater numbers of HU are needed. Such investigations are currently underway in our laboratory. Estimation of R_1, R_2, and TSR and inhibition by BBR might yield more information and shed light on the mechanisms underlying urate underexcretion, which would also facilitate an understanding of the pathophysiology of urate underexcretion among individual HU in medical practice.

Conclusion

To estimate urate transport contents in nephrons, the equation $C_{ua} = \{C_{cr}(1 - R_1) + TSR\}(1 - R_2)$ was designed and high-density regions with respect to the projection onto a coordinate axis of points at regular intervals on contour lines of this equation were investigated on graphs for two of three unknowns (R_1, R_2, and TSR). TSR was found to approximately correspond to C_{ua}BBR(●●), which could be determined by the BBR-loading C_{ua} test. UGF, UR_1, UTS, UR_2, and U_{ex} were approximated as 9,610; 9,510; 4,490; 4,150, and 440 μg/min in HU and 6,890; 6,820; 4,060; 3,610, and 520 μg/min in NC, respectively. Decreased TSR in HU was suspected as a fundamental change in terms of a high incidence of low TSR cases and high rate of decrease in TSR, as well as the pathophysiology of urate underexcretion. Increased UR_2 was considered to be the main cause of urate underexcretion in HU.

Acknowledgments

This work was supported in part by a grant-in-aid from the Gout Research Foundation of Japan. We wish to thank Prof. Akira Nakamura, Institute of Higher Education Research and Practice, Osaka University, for useful discussions regarding mathematical calculations, Mr. Naoki Okabayashi and Mr. Takeshi Tazima, Hayashi General Hospital, for their assistance with computer graphic figure formations, and Ms. Noriko Tamezawa and Ms. Akiko Ohno, Hayashi General Hospital, for their technical assistance in BBR-loading C_{ua} tests.

References

1 Maesaka JK, Fishbane S: Regulation of renal urate excretion: a critical review. Am J Kidney Dis 1998; 32:917–933.
2 Sica DA, Schoolwerth AC: Renal handling of organic anions and cations. Excretion of uric acid; in Brenner BM (ed): The Kidney. Philadelphia, Saunders, 1996, pp 680–700.
3 Sperling O: Hereditary renal hypouricemia; in Scriver CR, Beaudet AL, Sly WS, Valle D (eds): The Metabolic Basis of Inherited Diseases. New York, McGraw-Hill, 1989, pp 2605–2617.
4 Weinman EJ, Steplock D, Sansom SC, Knight TF, Senekjian HO: Use of high-performance liquid chromatography for determination of urate concentrations in nanoliter quantities of fluid. Kidney Int 1981;19:83–85.
5 Bordley J III, Richards AN: Quantitative studies of the composition of glomerular urine. J Biol Chem 1933;101:193–221.
6 Roch-Ramel F, Diezi-Chomety F, De Rougemont D, Tellier M, Wid-Mer J, Peters G: Renal excretion of uric acid in the rat: a micropuncture and microperfusion study. Am J Physiol 1976;230: 768–776.

7 Abramson RG, Lipkowitz MS: Evolution of the uric acid transport mechanism in vertebrate kidney; in Kinne RKH, Kinne-Saffran E, Beyenbach KW (eds): Basic Principles in Transport. Molecular Comparative Physiology. Basel, Karger, 1990, vol 3, pp 115–153.
8 Levinson DL, Sorensen LB: Renal handling of uric acid in normal and gouty subjects: evidence for a four-component system. Ann Rheum Dis 1980;39:173–179.
9 Diamond HS, Paolino JS: Evidence for a postsecretory reabsorptive site for uric acid in man. J Clin Invest 1973;52:1491–1499.
10 Steele TH, Boner G: Origins of the uricosuric response. J Clin Invest 1973;52:1368–1375.
11 Rieselbach RE, Steele TH: Influence of the kidney upon urate homeostasis in health and disease. Am J Med 1974;56:665–675.
12 Weinman EJ, Eknoyan G, Suki WN: The influence of the extracellular fluid volume on the tubular reabsorption of uric acid. J Clin Invest 1975;55:283–291.
13 Roch-Ramel F, Weiner IM: Excretion of urate by the kidney of Cebus monkeys: a micropuncture study. Am J Physiol 1973;224:1369–1374.
14 Diamond HS: Interpretation of pharmacologic manipulation of urate transport in man. Nephron 1989;51:1–5.
15 Rieselbach RE, Sorensen LB, Shelp WD, et al: Diminished renal urate secretion per nephron as a basis for primary gout. Ann Intern Med 1970;73:359–366.
16 Nakamura T, Tanaka T, Takagi K, Nakayama T, Inai K, Tsutani H, Ueda T: Urate transport in nephrons of gouty patients: quantitative analysis of urate transport in nephrons. Clin Exp Nephrol 1999;3:169–174.
17 Holmers EW, Kelley WN, Wyngaarden JB: The kidney and uric acid excretion in man. Kidney Int 1972;2:115–118.
18 Kahn AM: Effect of diuretics on the renal handling of urate. Semin Nephrol 1988;8:305–314.
19 Weiner IM: Urate transport in the nephron. Am J Physiol 1979;237:F85–F92.
20 Enomoto A, Kimura H, Chairoungdua A, et al: Molecular identification of a renal urate-anion exchanger that regulates blood urate levels. Nature 2002;417:447–452.
21 Ichida K, Hosoyamada M, Hisatome I, et al: Clinical and molecular analysis of patients with renal hypouricemia in Japan – influence of URAT1 gene on urinary urate excretion. J Am Soc Nephrol 2004;15:164–173.
22 Bahn A, Hagos Y, Reuter S, et al: Identification of a new urate and high affinity nicotinate transporter, hOAT10 (SLC22A13). J Biol Chem 2008;283:16332–16341.
23 Rizwan AN, Burkhardt G: Organic anion transporters of the SLC22 family: biopharmaceutical, physiological, and pathological roles. Pharm Res 2007;24:450–470.
24 Anzai N, Kanai Y, Endou H: Organic anion transporter family: current knowledge. Pharmacol Sci 2006;100:411–426.
25 Imamura S, Nakamura T: Characteristic features in pathophysiology of hyperuricemia with overproduction in gout. Purine Pyrimidine Metab 1994;18:132–143.
26 Nakamura T, Uchida M, Uchino H, Higuchi T: Studies on hyperuricemia of gout by means of the uric acid clearance. Uric acid metabolism in hyperuricemia of gout. Uric Acid Res 1977;1:45–61.
27 Weinman EJ, Sanson SC, Steplock DA, Sheth AU, Knight TF, Senekjian HO: Secretion of urate in the proximal convoluted tubule of the rat. Am J Physiol 1980;239:F383–F387.
28 Enomoto A, Endou H: Roles of organic anion transporters (OATs) and a urate transporter (URAT1) in the pathophysiology of human disease. Clin Exp Nephrol 2005;9:195–205.
29 Kramp RA, Lenoir R: Distal permeability to urate and effects of benzofuran derivatives in the rat kidney. Am J Physiol 1975;228:875–883.
30 Vitart V, Rudan I, Hayward C, et al: SLC2A9 is a newly identified urate transporter influencing serum urate concentration, urate excretion and gout. Nat Genet 2008;40:437–442.
31 Diamond HS, Paolino JS: Evidence for a postsecretory reabsorptive site for uric acid in man. J Clin Invest 1973;52:1491–1499.
32 Fanelli GM Jr, Weiner IM: Pyrazinoate excretion in the chimpanzee. J Clin Invest 1973;52:1946–1957.
33 Spering O: Hereditary renal hypouricemia; in Scriver CR, Beaudet AL, Sly WS, Valle D (eds): The Metabolic Basis of Inherited Diseases, ed 6. Tokyo, McGraw-Hill, 1960, pp 2605–2617.
34 Roch-Ramel F, Guisan B: Renal transport of urate in humans. News Physiol Sci 1999;14:80–85.
35 Becker MA: The biochemistry of gout; in Wortmann RL, Schumacher R Jr, Becker MA, Ryan LM (eds): Crystal-Induced Arthropathies: Gout, Pseudogout and Apatite-Associated Syndromes. New York, Taylor & Francis, 2006, pp 189–212.